Mode coupling in a vibronic laser

F. Marquis
Centre d'Applications Laser, Ecole Polytechnique Fédérale, 1015 Lausanne, Switzerland

P. Schwendimann
Defense Technology and Procurement Agency, System Analysis Division, 3000 Bern 25, Switzerland
(Received 19 July 1988)

Taking into account the vibronic-level structure in a laser medium, we study the influence of electron-vibration interaction on the field dynamics. Different vibronic transitions are coupled in the medium through this interaction and contribute to the emission from excited states, thus coupling different field modes in the cavity and influencing the field dynamics. A general model is presented and solved in a simple example of four coupled transitions. In particular, the effect of degenerate transitions is stressed.

I. INTRODUCTION

In the last few years, tunable infrared solid-state lasers as well as molecular lasers have been the object of rapid development.[1] As it is well known, they exploit the transitions between vibronic states in impurities embedded in a host crystal or in gas molecules. The main characteristics of these systems (gain, threshold, etc.) have already been modeled in Ref. 2. This approach has the advantage of giving an explicit account of the influence of the interaction between electrons and vibrations (e.g., electron-phonon interaction in a solid-state laser) on the laser characteristics. Therefore, an "*ab initio*" description of laser action in a vibronic system is obtained, which does not rely on the useful but rather *ad hoc* three- or four-level transition scheme.

In Ref. 2, the basic elements of the theory of the vibronic laser have been presented, with emphasis on the influence of the electron-vibration interaction on the laser parameters. In this paper we go one step further and discuss the consequences of the peculiar features of the vibronic spectrum on the laser dynamics. We have chosen to work with a small number of vibronic levels, in order to have a quick insight into the dynamical behavior of these systems. Furthermore, in our numerical examples, we use values for the different parameters (coupling constants, frequencies, etc.) which fit well with that of a molecular laser, such as, for example, XeCl. We want, however, to stress that we are not trying to link our results with a definite experimental situation. In this sense this choice has merely an illustrative character.

We focus in this paper on two main points, and organize it as follows. First of all we investigate in a general case the dynamical relevance of the mode coupling induced by resonant coupling to different vibronic transitions, which has been put in evidence in Ref. 2. We then show in a first example how the emitted intensity is distributed between the different modes, depending on the strength of the coupling between different transitions and on the excitation (pump) parameter, when only one excited state is present. Furthermore, since transitions between different pairs of vibronic states having the same frequency are possible, we discuss in a second example how this frequency degeneracy changes the redistribution of the intensity between different modes, in the case where two excited states are present. We stress the fact that results presented here are characteristic of any vibronic system and show up independently of the number of states involved in the computation.

II. MODEL EQUATIONS

The vibronic laser model which we use here has already been discussed in detail.[2,3] Therefore, we will here only summarize its main features. As a consequence of the interaction of two electronic states with a vibrational field, the level structure of the system shows the characteristics represented in Fig. 1. Here the electron-vibration coupling is assumed to be linear and only optical phonons are considered. The laser transitions occur between upper vibronic levels m in the upper potential sheet, lower levels n belonging to the lower potential sheet. Besides these transitions, which are characterized by raising (S_{mn}^{+}) and lowering (S_{mn}^{-}) operators below, we consider also transitions between vibronic states in the same potential sheet, which are described, respectively, by T_{ln}^{+} and T_{ln}^{-} operators. Here the + and − signs indicate that the transition takes place in the upper or lower potential sheet. The T_{kl}^{+} with equal indices describe the population of the corresponding state. Replacing the operators with their expectation values on a suitable initial state, and expressing the polarization through S_{mn}^{+} and S_{mn}^{-}, the semiclassical laser equations are given by

$$\frac{d}{dt}S_{mn}^{+} = -\gamma_{mn}S_{mn}^{+} + i[\varepsilon - \Omega(n-m)]S_{mn}^{+} - i\sum_{k,l} g_k a_k^{+}(f_{ln}T_{ml}^{+} - f_{ml}T_{ln}^{-}) , \tag{2.1}$$

where a_k are the classical electromagnetic field modes. The equation for S_{mn}^{-} is obtained by taking the complex

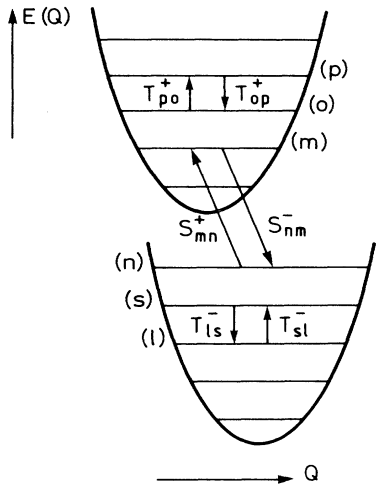

FIG. 1. Vibronic-level structure for the case of two electronic states. E is the energy and Q is a phonon-configuration coordinate proportional to the displacement $(b+b^+)$

conjugate of (2.1) and interchanging the order of the indices in the expression. For the inversion $I_{mn}=T^+_{mm}-T^-_{nn}$ we obtain

$$\frac{d}{dt}I_{mn}=-\gamma^T_{mm}I_{mn}+\gamma^T_{mm}\Delta N_{mn}+i\sum_{k,l}g_k[(f_{nl}S^-_{nl}+f_{lm}S^-_{lm})a^+_k-(f_{ml}S^+_{ml}+f_{ln}S^+_{ln})a_k]\ , \tag{2.2}$$

where $\Delta N_{mn}=(T^+_{mm}-T^-_{nn})^0$ is the pump source term. The nondiagonal quantities $T^\pm_{mn}$ obey

$$\begin{aligned}\frac{d}{dt}T^+_{mn}&=-[\gamma^+_{mn}+i\Omega(n-m)]T^+_{mn}-i\sum_{k,l}g_k(f_{nl}S^+_{ml}a_k-f_{lm}S^-_{ln}a^+_k)\ ,\\ \frac{d}{dt}T^-_{mn}&=-[\gamma^-_{mn}+i\Omega(n-m)]T^-_{mn}+i\sum_{k,l}g_k(f_{lm}S^+_{ln}a_k-f_{nl}S^-_{ml}a^+_k)\ .\end{aligned} \tag{2.3}$$

Finally, the classical field modes are described by

$$\begin{aligned}\frac{d}{dt}a_k&=-\Gamma a_k-i\omega_k a_k-i\sum_k\sum_{m,n}g_k f_{nm}S^-_{nm}\ ,\\ \frac{d}{dt}a^+_k&=-\Gamma a^+_k+i\omega_k a^+_k+i\sum_k\sum_{m,n}g_k f_{mn}S^+_{mn}\ .\end{aligned} \tag{2.4}$$

The quantities $\gamma^\pm_{mn}$, γ_{mn}, and γ^T_{mm} are damping constants for the transitions between levels belonging, respectively to the same potential sheet and different sheets, and Γ is the damping constant for the field modes a_k. The quantities f_{nm} are the Frank-Condon overlap integrals which characterize the transition between upper and lower levels and depend on the strength of the electron-vibration coupling. Their explicit expression is found in Ref. 2 or in standard literature.[4] Finally, the g_k are the dipole-coupling constants to the electronic transitions and Ω and ε are the vibration and electron transition frequencies, respectively. ω_k is the frequency of mode k. For more details on this model, the reader is referred to Ref. 2.

The material equations (2.1)–(2.3) are then solved by perturbation calculation around threshold in the spirit of Lamb's semiclassical laser theory.[5] As a zeroth-order approximation, the unsaturated populations are used, whereas all other quantities are zero. After some straightforward algebra, the contribution to the polarization up to third order in the electromagnetic field is given by

$$\begin{aligned}(S^+_{mn})^{(3)}=4i\sum_k g_k^3|A_k|^2A_k^*\frac{f^4_{mn}}{\gamma^2_{mn}\gamma^T_{mm}}e^{-i(\omega_k+\phi_k)t}\\ +\sum_{k,k'(k\neq k')}g_k^2g_k|A_{k'}|^2A_k^*\frac{f_{mn}}{\gamma_{mn}}\\ \times e^{-i(\omega_k+\phi_k)t}(\alpha_1+\alpha_2)\ ,\end{aligned} \tag{2.5}$$

with α_1 and α_2 defined as

$$\alpha_1=f_{mn}\sum_l f_{lm}\Delta N_{ml}\left[\frac{1}{\gamma_{lm}}\left[\frac{1}{\gamma_{lm}}+\frac{1}{\gamma^T_{ll}}\right]\right]\ ,$$

$$\alpha_2=\sum_{l,l'}\frac{1}{\gamma_{lm}+i(l-m)\Omega}f_{ll'}\left[\frac{\Delta N_{ml'}f_{ml'}}{g_{l'm}}+\frac{\Delta N_{l'l}f_{l'm}}{\gamma_{ll'}}\right]+\sum_{l,l'}\frac{1}{\gamma_{nl'}+i(l'-n)\Omega}f_{ll'}\left[\frac{\Delta N_{l'n}f_{l'n}}{g_{nl'}}+\frac{\Delta N_{l'l}f_{nl'}}{\gamma_{ll'}}\right]\ .$$

We have used $a_k=A_k(t)\exp[i(\omega t+\phi_k t)]$. Here only the terms which correspond to resonant transitions have been retained and we assume that two mode indices are equal. In (2.5) we recognize two sorts of "resonant" terms: terms which do not contain a dependence on the vibration frequency Ω in the denominator and terms which depend on the frequency difference $(m-n)\Omega$ between vibronic states. Let us discuss these different contributions in more detail. The vibration-independent terms contain self-saturation contribution to a single mode, originating from the inversion terms as in the usual two-level theories, as well as terms coupling different modes through different transitions. The latter terms are peculiar of the vibronic laser model of Ref. 2, and are not present in the simple two-level atom theory. (This shows why such a simple model is not able to cope with vibronic lasers.) The phonon-frequency-dependent terms also contain both kinds of coupling. However, they originate mainly from the population terms in the perturbation development. Their contribution to the transition rate should be of minor importance since the denominator terms turn out to be larger than those of the frequency-independent terms. Here we have displayed these terms, which had been disregarded in Ref. 2, for the sake of completeness.

In order to simplify the discussion of the dynamics involved by (2.4) and (2.5), we now limit ourselves to a situation in which at most four lower levels and two upper levels are present. Furthermore, we neglect the terms depending on $(m-n)\Omega$ in the following. Within this assumption the field equations become

$$\frac{d}{dt}|A_k| = -\Gamma|A_k| - \frac{g_k^2 f_{mn}^2}{\gamma_{mn}}\Delta N_{mn}|A_k| - \frac{8g_k^4 f_{mn}^4 |A_k|^3}{\gamma_{mn}^2 \gamma_{mm}^T}\Delta N_{mn}$$
$$-2g_k^2|A_k|\frac{f_{mn}^2}{\gamma_{mn}}\sum_{k'(k'\neq k)} g_{k'}^2|A_{k'}|^2 \sum_l f_{ml}^2 \frac{1}{\gamma_{ml}}\left[\frac{1}{\gamma_{ml}} + \frac{1}{\gamma_{mm}^T}\right]\Delta N_{ml}\ , \tag{2.6}$$

where m takes the values 1 and 2, and l and n range from 1 to 4.

III. COUPLED TRANSITION DYNAMICS

The number of possible transitions in a vibronic system being very large, we have decided, as we already anticipated to limit the number of intervening vibronic levels. This number is kept small enough so that the mechanism of the coupling and the main features of a vibronic laser are revealed, at least in the approximation expressed by (2.5). In the following we discuss two different configurations. In the first example, one excited upper level is coupled to four lower levels. The second configuration consists of two excited upper levels coupled to two lower levels, thus containing a double transition which is degenerate in frequency. We will show that the presence of these degenerate transitions strongly influences the laser dynamics.

A. One upper level

The equations for the intensities of the four coupled modes are

$$\frac{d}{dt}I_k = 2I_k\left[A_k + B_k I_k + \sum_{k(\neq k')} C_{kk'} I_{k'}\right]\ , \tag{3.1}$$

with $k,k' = 1,2,3,4$, where

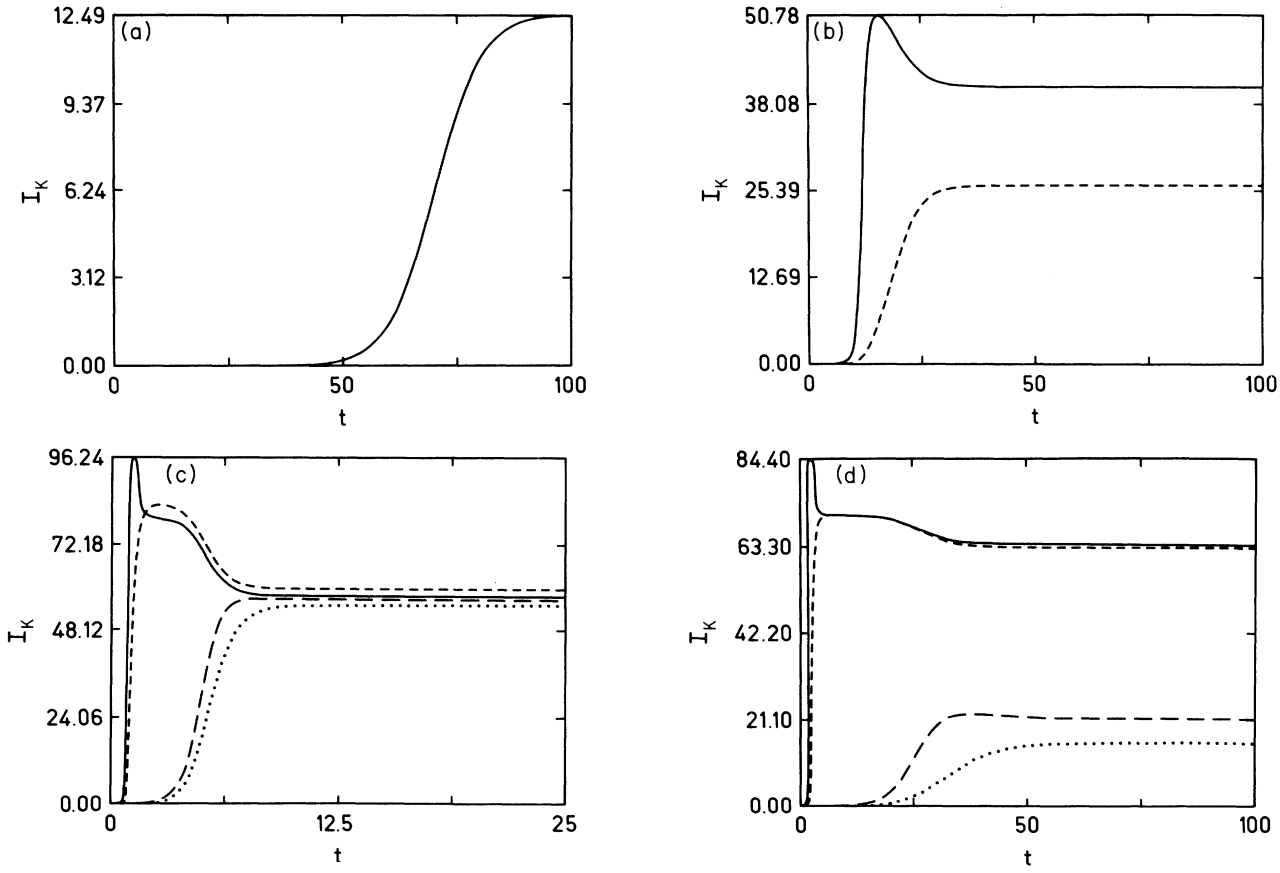

FIG. 2. Coupled intensities I_k as a function of time for the case where only the fundamental vibronic level is populated in the upper potential sheet, and four vibronic levels are considered in the lower potential sheet. The intensities are represented in arbitrary units for different values of the pump parameter N/N_T. t is normalized to $\Omega/2Q$, where Q is the quality factor of the cavity. The different curves correspond, respectively, to $k=1$ (dotted line), $k=2$ (solid line), $k=3$ (short-dashed line), and $k=4$ (long-dashed line). (a)–(d) display the coupled intensities for N/N_T equal to, 1.1, 1.6, 9.1, and 4.5, respectively. (Note that the medium parameters are pertinent to a molecular XeCl laser.)

$$A_k=\omega_k\left[\frac{N}{N_T}\frac{f_{mn}^2}{f_{01}^2}-1\right],$$

$$B_k=-\omega_k\frac{N}{N_T}\frac{\gamma_{00}^T}{4\gamma_{mm}^T}\frac{f_{mn}^4}{f_{01}^2}, \tag{3.2}$$

$$C_{kk'}=-\omega_k\frac{N}{N_T}\frac{\gamma_{00}^T}{8}\left[\frac{1}{\gamma_{mn}}+\frac{1}{\gamma_{mm}^T}\right]\frac{f_{mn}^2 f_{mn'}^2}{f_{01}^2},$$

with $n=k-1$, $n'=k'-1$, and $m=0$. N is the excited-center density, and N_T is the threshold value for laser action in the stronger transition (in our case $m=0\rightarrow n=1$) expressed by

$$N_T=\frac{\varepsilon_0\hbar\gamma_{00}^T}{g_k^2\Gamma f_{01}^2}.$$

The equations are solved numerically as a function of time. We expect to find a dynamical behavior analogous to that of a standard two-level system coupled to different modes. However, we stress the fact that in our case the mode coupling is determined by the Frank-Condon factors (i.e., the electron-vibration coupling), and is in fact a "transition" coupling. In contrast to the two-level system, the coupling here is resonant, and the conditions for mode oscillation are influenced by electron-vibration coupling only. Therefore, it is of interest to briefly discuss these results. Figure 2 displays the coupled-transition dynamics for different values of the parameter N/N_T. As one expects, for low values of N/N_T, the mode corresponding to the strongest transition starts to oscillate [Fig. 2(a)]. When increasing N/N_T, the other transitions become active, too [Fig. 2(b)], in a sequence given by the strength of their respective Frank-Condon factors, i.e., in our example transitions from $m=0$ to $n=2$, $n=3$, and finally $n=0$, for decreasing values of f_{mn}. When all transitions are above threshold, there is a remarkable redistribution of the intensity between the different coupled transitions. This redistribution can lead to different situations, where, for example, the four intensities can be almost equal [Fig. 2(c)], or on the contrary where one specific mode can dominate [Fig. 2(d)]. Note that the strongest mode does not always correspond to the strongest transition. In order to test our results, we have also done some computations by retaining nonresonant terms, which are not written explicitly in (2.5). This calculation is principally done in order to see whether the mode-mode coupling contribution due to nonresonant coupling of two modes to the same transitions may become competitive with the resonant transition coupling. The result of our computations leads to the conclusion that introducing the closest nonresonant contributions in the evaluation of the gain and saturation coefficients does not induce any noticeable change of the time evolution of the intensities. This means that, in this example, the contributions of nonresonant mode-mode coupling are negligible compared to the resonant contributions.

Finally, the time evolution of the phases determines the phase shift. The nonlinear contributions to this shift are very small. An example shows that this intracavity intensity-dependent shift is about 100 times smaller than the frequency difference between two neighboring eigenmodes of the empty cavity.

B. Two excited upper levels

When more than one upper level is excited, frequency-degenerate transitions, i.e., transitions with the same frequency but connecting different levels are present. We consider a simple case where four levels are present, two in each potential sheet. The vibration frequency Ω being the same in the two sheets, two transitions are degenerate and contribute to the same mode of the cavity field. Thus the four transitions considered in this example correspond to only three modes of the field. We characterize them by their indices k, defining $k=1$ and $k=3$ as the modes corresponding to the nondegenerate transitions $m=0\rightarrow n=1$, and $m=1\rightarrow n=0$, respectively. Their Frank-Condon factors are equal and larger than the factors characterizing the degenerate transitions ($m=n=1$, and $m=n=0$). These, on the other hand, contribute to mode $k=2$. They are characterized by smaller Frank-Condon factors, f_{00} being, however, still larger than f_{11}. Once more we numerically solve the coupled equations (3.1) for the intensities. However, the coefficients for the degenerate mode are now redefined as

$$A_2=\omega_2\left[\frac{N}{N_T}\frac{f_{00}^2+f_{11}^2}{f_{01}^2}-1\right],$$

$$B_2=-\omega_2\frac{N}{N_T}\frac{\gamma_{00}^T}{4\gamma_{mm}^T}\frac{f_{00}^4+f_{11}^4}{f_{01}^2},$$

$$C_{12}=-\omega_1\frac{N}{N_T}\frac{\Gamma}{8}\left[\frac{1}{\gamma_{mn}}+\frac{1}{\gamma_{mn}^T}\right](f_{00}^2+f_{11}^2).$$

The remaining coefficients are deduced from these as $C_{21}=C_{23}=C_{12}(\omega_2/\omega_1)$, $C_{32}=C_{12}(\omega_3/\omega_1)$. Here the normalization is given by the largest of the Frank-Condon factors in play, in our example, f_{01}. Modes 1 and 3 are coupled to mode 2 only ($C_{12}\neq 0$ and $C_{32}\neq 0$); since only resonant terms are considered, they are not coupled together ($C_{13}=0$).

To discuss the dynamical behavior of the coupled modes, we distinguish between a symmetric-pumping and an asymmetric-pumping configuration. Symmetric pumping populates both upper levels equally. The time-dependent intensities are shown in Fig. 3. The nondegenerate transitions oscillate above their threshold values, whereas the degenerate transitions are inhibited. This is explained as follows; in the chosen configuration, the Frank-Condon factors of both nondegenerate transitions happen to be larger than the degenerate ones; therefore, their thresholds are lower. Hence we are in a situation which is reminiscent of that of the many-mode two-level model where the strongest modes (i.e., the modes with lower threshold) oscillate at the expense of the other.

The case of asymmetric pumping, characterized by a situation where the higher of the two upper levels is less populated than the lower one, leads to a different behavior. We discuss it by introducing the pump ratio r, where

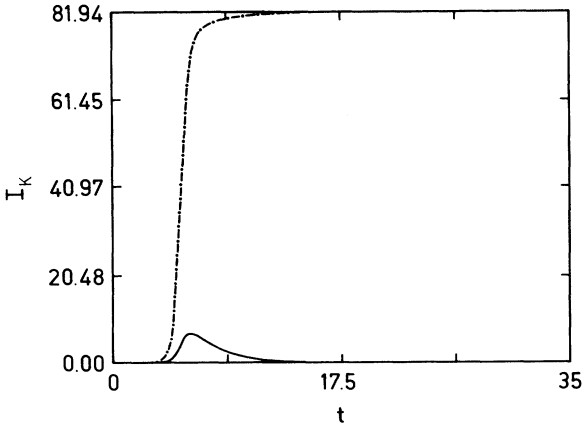

FIG. 3. Intensities of the coupled modes I_k as a function of time, for symmetric pumping, $N/N_T=2.5$. Two vibronic levels are considered in each potential sheet; mode $k=2$ corresponds to two degenerate transitions. The different curves correspond, respectively, to $k=1$ (dotted line), $k=2$ (solid line), and $k=3$ (dashed line).

r is the ratio of the pump in the upper level $m=1$ to the pump in the upper level $m=0$,

$$r=\frac{N(m=1)}{N(m=0)}\ ,$$

and varying r for a fixed value of N/N_T. For small r, the higher upper level is almost empty, and competition between transitions $m=0\rightarrow n=1$ and $m=0\rightarrow n=0$ occurs [Fig. 4(a)]. Increasing r for the same value of N/N_T the contribution of the transition $m=1\rightarrow n=1$ to the degenerate mode $k=2$ increases, leading to a stronger competition between modes 1 and 2. Mode 2 consequently increases at the expense of mode 1 [Fig. 4(b)]. Further increase of r leads to a stronger effect of transition $m=1\rightarrow n=0$, then to the appearance of the third mode [Fig. 4(c)], and finally to the inhibition of oscillation of mode 2 for symmetric pumping, when the contribution of the nondegenerate transition becomes large enough. Note that in all this discussion, the pump N/N_T is kept constant, and that only the relative pump into the two upper levels determines which will be the strongest oscillating mode. On the other hand, when r is fixed and N/N_T is varied, the three modes can oscillate simultaneously, starting with oscillation of mode 1 for low values of the pump followed by the appearance of mode 2 competing with 1 for larger values of the pump, and finally simultaneous oscillation of the three modes, with redistribution of the energy for even larger values of the global pump.

This phenomenological discussion shows that due to the coupling between the transitions induced by electron-vibration interaction in the medium, the dynamics of a vibronic laser is much richer than that of a standard two-level system, and can be correctly described only by a model that takes into account the presence of the coupled set of vibronic states associated with each electronic state. Depending on the strength of the interaction, the lasing mode can actually be shifted from the strongest transition in the fluorescence spectrum of the laser medium towards a different weaker transition, whose contribution is somehow reinforced by the coupling. Furthermore, the degeneracy in frequency, which appears as soon as more than one upper level is excited, allows the reinforcement of transitions having a smaller gain. This effect may be of some experimental interest

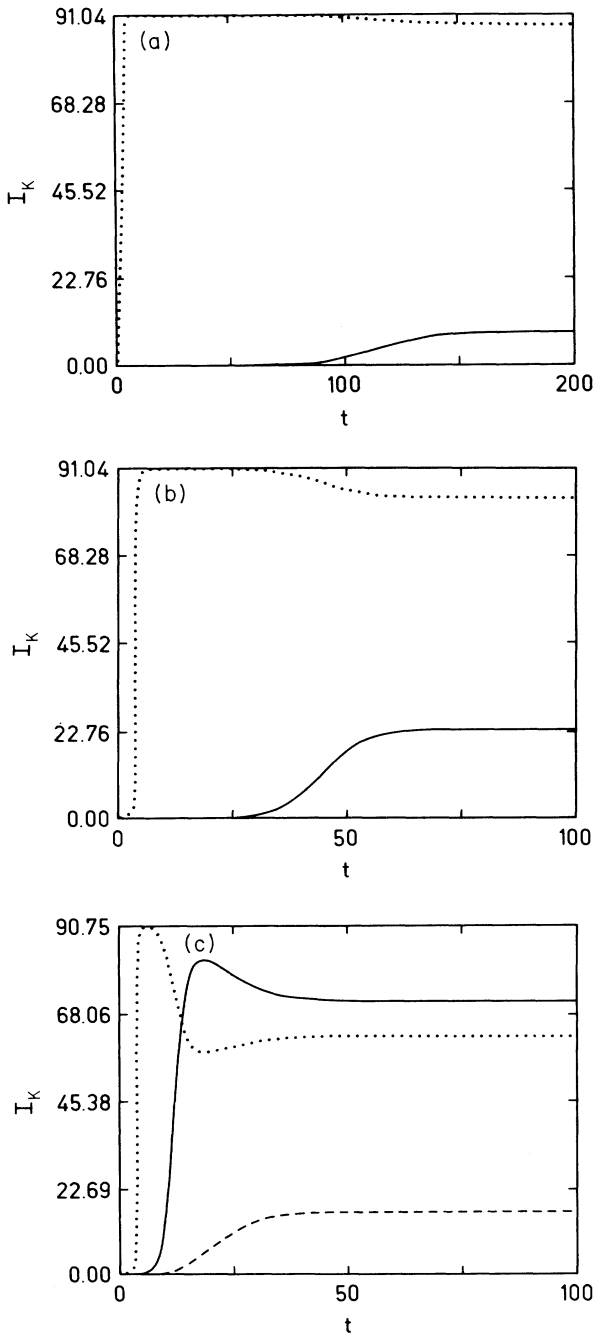

FIG. 4. Same as Fig. 3, for the case of asymmetric pumping. N/N_T is kept constant in all the figures, and equal to 3. (a)–(c) display different values of the relative pump r, $r=\frac{1}{200}$, $\frac{1}{10}$, and $\frac{1}{2}$, respectively.

because the asymmetrical pumping configuration discussed above is more likely to be obtained when equilibrium between inversion and pump mechanism is established.

In conclusion, we have given a first simplified picture of the dynamics of the interaction between light and a pumped vibronic system, which has a richer structure than the usual atomic systems. The interplay between coupled modes and transitions allows for new effects (such as the dynamical influence of transitions which are degenerate in frequency) which may be of practical relevance.

ACKNOWLEDGMENT

One of the authors (P.S.) acknowledges the kind hospitality of the Centre d'Applications Laser, where part of this work was done.

[1]H. J. Paus, *Physics and Chemistry of Solids* (Polish Academy of Sciences, Wroclaw, 1986), p. 69, and references therein; in *Tunable Solid State Lasers, Proceedings of the First Conference on Tunable Solid State Lasers, La Jolla,* edited by P. Hammerling *et al.* (Springer, Berlin, 1985); IEEE J. Quantum Electron. **QE-21**, 1554 (1985); J. Opt. Soc. Am. **3** (1), 81 (1986); H. Durr, Laser Optoelektron. **15**, 31 (1983); R. Florian, L. D. Schwan, and D. Schmid, Phys. Rev. A **29**, 2709 (1984); in *Excimer Lasers,* edited by CH. K. Rhodes (Springer-Verlag, Berlin, 1984).

[2]P. Schwendimann, E. Sigmund, and K. Zeile, Phys. Rev. A **37**, 3018 (1988).

[3]E. Sigmund and P. Schwendimann, Opt. Acta **32**, 281 (1985); P. Schwendimann and E. Sigmund, Solid State Commun. **50**, 379 (1984).

[4]M. Wagner, Z. Naturforsch. **14**A, 81 (1959); S. Koide, *ibid.* **15**A, 123 (1960).

[5]W. E. Lamb, Jr., Phys. Rev. **137**, A1429 (1964).